



Optimising position control of a solar parabolic trough

Authors:

Puramanathan Naidoo¹
Theo I. van Niekerk²

Affiliations:

¹Electrical Engineering,
Mangosuthu University of
Technology, Durban,
South Africa

²Mechatronic Engineering,
Nelson Mandela
Metropolitan University,
Port Elizabeth, South Africa

Correspondence to:

Puramanathan Naidoo

email:

pnaidoo@mut.ac.za

Postal address:

PO Box 12363, Jacobs
4026, Durban, South Africa

Dates:

Received: 01 June 2009

Accepted: 02 Feb. 2011

Published: 16 Mar. 2011

How to cite this article:

Naidoo P, Van Niekerk TI.
Optimising position control
of a solar parabolic trough.
S Afr J Sci. 2011;107(3/4),
Art. #452, 6 pages. DOI:
10.4102/sajs.v107i3/4.452

In today's climate of growing energy needs and increasing environmental concerns, alternatives to the use of non-renewable and polluting fossil fuels have to be investigated. One such alternative is solar energy. This study is based on the implementation of a mathematical computation – the PSA (Plataforma Solar de Almeria) computation developed at PSA (the European Test Centre for solar energy applications) – embedded in a control algorithm to locate the position of the sun. Tests were conducted on a solar parabolic trough (SPT) constructed at the Solar Thermal Applications Research Laboratory of the Mangosuthu University of Technology (Durban, South Africa) for optimal position control using the PSA value. The designed control algorithm embedded in an industrial Siemens S7-314 C-2PtP programmable logic controller compared the PSA computation to a measured position of the SPT to optimally rotate the SPT to a desired position with the constant movement of the sun. The two main angles of the sun relative to the position of the SPT on earth, the zenith angle and the azimuth angle, both calculated in the PSA from the vertical and horizontal planes, respectively, were applied to the control algorithm to generate an appropriate final tracking angle within a 0.007 radian (0° 24' 3.6") tolerance, in accordance to the construction specifications and solar collector testing standards of the American Society of Heating, Refrigerating and Air-Conditioning Engineers (ASHRAE, 1991). These values, together with the longitude and latitude applicable to the geographical location of the SPT, were processed in the control software to rotate the SPT to an optimal position with respect to the position of the sun in its daily path, for solar-to-thermal conversion.

Introduction

A solar parabolic trough (SPT) is a linear solar collector with, as its name implies, a parabolic cross section. Its reflective surface concentrates sunlight onto a receiver tube located along the trough's single horizontal focal line, therefore tracking the sun along only one axis, either north–south or east–west.^{1,2,3} A north–south orientation provides slightly more energy per year than an east–west orientation, but its winter output is low in mid-latitudes whereas an east–west orientation provides a more constant output throughout the year.⁴ The SPT at STARlab was constructed and installed in a north–south position to track the sun in an east–west direction, referred to as a one-axis SPT. A two-axis SPT has the disadvantage of losing thermal energy and is not cost effective. Each parabolic trough collector and its associated receiver tube, tracking device and controls form a modular collector assembly that can be connected in various series or parallel-flow circuits to achieve a range of performance characteristics. Solar tracking is particularly important in systems that operate under concentrated sunlight.^{1,5,6}

Energy losses arise from inefficient solar tracking and position control of the collector. Various factors may reduce the system output efficiency. The performance of a solar–thermal plant reflects the efficiency and reliability of its four principal systems, i.e. collector, receiver, transport–storage and conversion.⁷ The remaining sunlight is defined as the usable or available solar energy because some solar input is lost when the plant cannot operate. A certain amount of energy is lost at each processing stage, e.g. sunlight is lost in the collector system as a result of sun-angle effects and optical losses, thermal energy is lost in the receiver and heat-transport system, and a significant loss occurs in the conversion process. The efficiency of the collector system depends on the reflectivity of its mirrors and the optical effectiveness of its geometry. Losses in the system result from sun-angle effects (also called cosine losses), soiling of the mirrors, shadowing, optical losses at the receiver and blocking of sunlight from the reflective surface by other components, as well as spillage of reflected sunlight outside the receiver boundaries.^{8,9,10} Compensation in the calculated acute angle was required to generate a final angle to correctly position the trough in one of the four mathematical quadrants of the coordinate plane according to the tangent trigonometric ratio.¹¹

Method and materials

Experimental set-up

The set-up of the trough and fluid system comprised a receiver tube diameter of 25 mm and a collector area of 7.5 m² aperture (5.0 m x 1.5 m) (Figure 1). The fluid was pumped from the

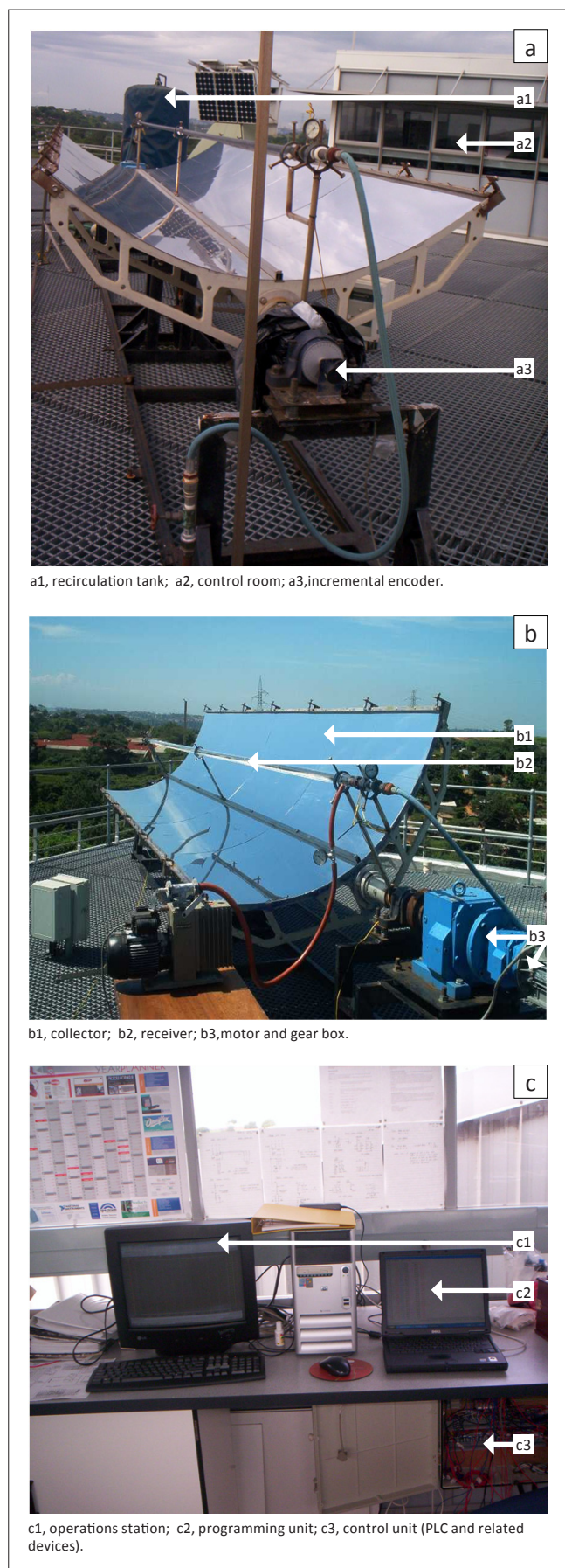


FIGURE 1: The experimental set-up of the solar parabolic trough: (a) the non-drive end, (b) the drive end and (c) the operations station, programming and control units in the control room.

recirculation tank through the receiver tube, allowing the radiation of the sun to be reflected from the collector surface onto the receiver tube. The amount of reflected radiation from the available radiation was determined by the position of the SPT driven by an induction motor and gearbox. Both the calculated position of the sun by the embedded Plataforma Solar de Almeria (PSA) computation and the measured position of the trough by the incremental encoder were applied as input data signals to the programmable logic controller (PLC) located in the control room. The signals were processed in the configured control algorithm to generate a corrective output data signal to rotate the SPT when required, to meet a specific tolerance range. The software program¹³ facilitated configuration of the control architecture and the control unit facilitated interfacing of field measuring and correcting instruments to the PLC hardware.

Establishing control aspects for optimal solar-to-thermal conversion

For optimal solar-to-thermal conversion, accurate tracking of the sun is required by the PSA computation relative to the critical positioning of the SPT by the control algorithm (Figure 2).¹² The SPT is rotated about its central axis by the motor, from the horizontal, 0-degree axis at sunrise (referred to as +90°), through the vertical, 90-degree axis at zenith (referred to as 0°), to the horizontal, 180-degree axis at sunset (referred to as -90°). For maximum absorption of solar radiation, the beam position should be perpendicular to the normal of the collector surface, within 7.0 milliradians (0° 24' 3.6") of striking the collector surface, according to mechanical design specifications.¹¹ The ideal position of the SPT relative to the sun for maximum solar-to-thermal conversion is at 'Y', the point where the beam position will be perpendicular to the normal of the collector surface. However, to meet the 7.0 milliradian tolerance, the sun should be located within positions 'X' and 'Z' in its path, i.e. 3.5 milliradians (0° 12' 1.8") on either side of the ideal position, as specified by tests conducted at PSA.¹³ Any positions outside of this range nullify the solar-to-thermal conversion for test purposes. The control strategy must ensure that misalignment of the SPT is avoided to prevent the sun position exceeding the 0.007 radian tolerance.¹¹

Developing the control algorithm to generate a calculated final angle of the SPT

Whilst the sun travels in its daily path, the PSA computation calculates a value representative of the position of the sun.¹² This value and the pulsed signal from the incremental encoder, representative of the SPT position, were applied as inputs to the summing point of the controller as pulse-count signals (Figure 3). A corrective signal was generated from the summing point of the controller to the motor, as an angular signal in radians, to continuously rotate the SPT to a new position as the sun revolves in its daily path at a rate of 0.25°/min; 0 pulses to 2500 pulses represent a 360-degree rotational movement. Because the trough rotates from sunrise to sunset, a movement of 180-degrees, the encoder operates for 1250 pulses. According

to the encoder specification, 2500 pulses per 360° equates to $0.144^\circ/\text{pulse}$. Incorporating the 0.007 radian tolerance, i.e. 0.401° (0.007×57.3), equates to 2.78 pulses ($0.401/0.144$). The control algorithm was configured to measure a three-pulse integer count, nearest to 2.78. This method was essential to avoid the problem of hysteresis in the software processing for the application by omitting fractions and decimals before rotating the SPT to maintain the required 0.007 radian tolerance angular position. Incorporating the 0.007 radian tolerance (0.401°), it was derived that $0.401/0.144 = 2.78$ pulses; therefore 2 pulses were applied in the software (i.e. $2 \text{ pulses} = 0.288^\circ$). Incorporating the sun's movement of $0.25^\circ/\text{min}$ ($0.00417^\circ/\text{s}$), it was derived that $0.288^\circ/0.00417^\circ/\text{s} = 69.06 \text{ s}$. Using the values calculated above (and assuming that the motor is ON for 4 s, based on an open-loop test using timers in the control software), the motor speed was determined as follows^{13,14,15}: $0.288^\circ/4 = 0.072^\circ/\text{s}$, and, because the gearbox has a 463:1 ratio, $0.072 \times 463 = 33.33^\circ/\text{s}$ (or 5.556 rpm). The motor speed was therefore 5.556 rpm.

The pulsed signal was applied to a quadruple counter in the software, converting the 1250-pulse signal to a 5000-pulse signal (2500 pulses on either side of the vertical) for higher bit-resolution in the digital controller, improving data processing to contribute to control optimisation. The trough at sunrise was

represented by +2500 pulses ($+90^\circ$), the trough at the vertical position was represented by 0 pulses (0°) and the trough at sunset was represented by -2500 pulses (-90°) (Figure 2). However, the control software was configured to the limits of +2600 pulses and -2600 pulses for technical considerations to prevent the SPT exceeding the maximum safety limits. The additional 100 pulses were assigned to prevent software conflict for uninterrupted operation if the SPT exceeded either the -90° or $+90^\circ$ positions.¹⁵

The incremental encoder generated three pulses, namely pulses A, B and C. Pulse A was active when there was rotational movement of the SPT (Figure 3); the specification of the pulse was determined by the speed at which the SPT rotated. Pulse B determined the direction of rotation of the SPT. If pulse B was in phase with pulse A, the SPT was rotating forward. Reverse rotation was detected by pulses A and B being out of phase with each other. Marker pulse C set the reference point to detect the 0° position of the trough. Pulse C commenced at logic 1 at the start of SPT movement (from sunrise) and remained at logic 1 until the vertical position of the SPT when it reached a transition state to logic 0. The same applied from the vertical to sunset positions. In the event of a power failure, marker pulse C made provision for the SPT to rotate to the zenith position and return to its operating position after power restoration, preventing software conflict.¹⁵

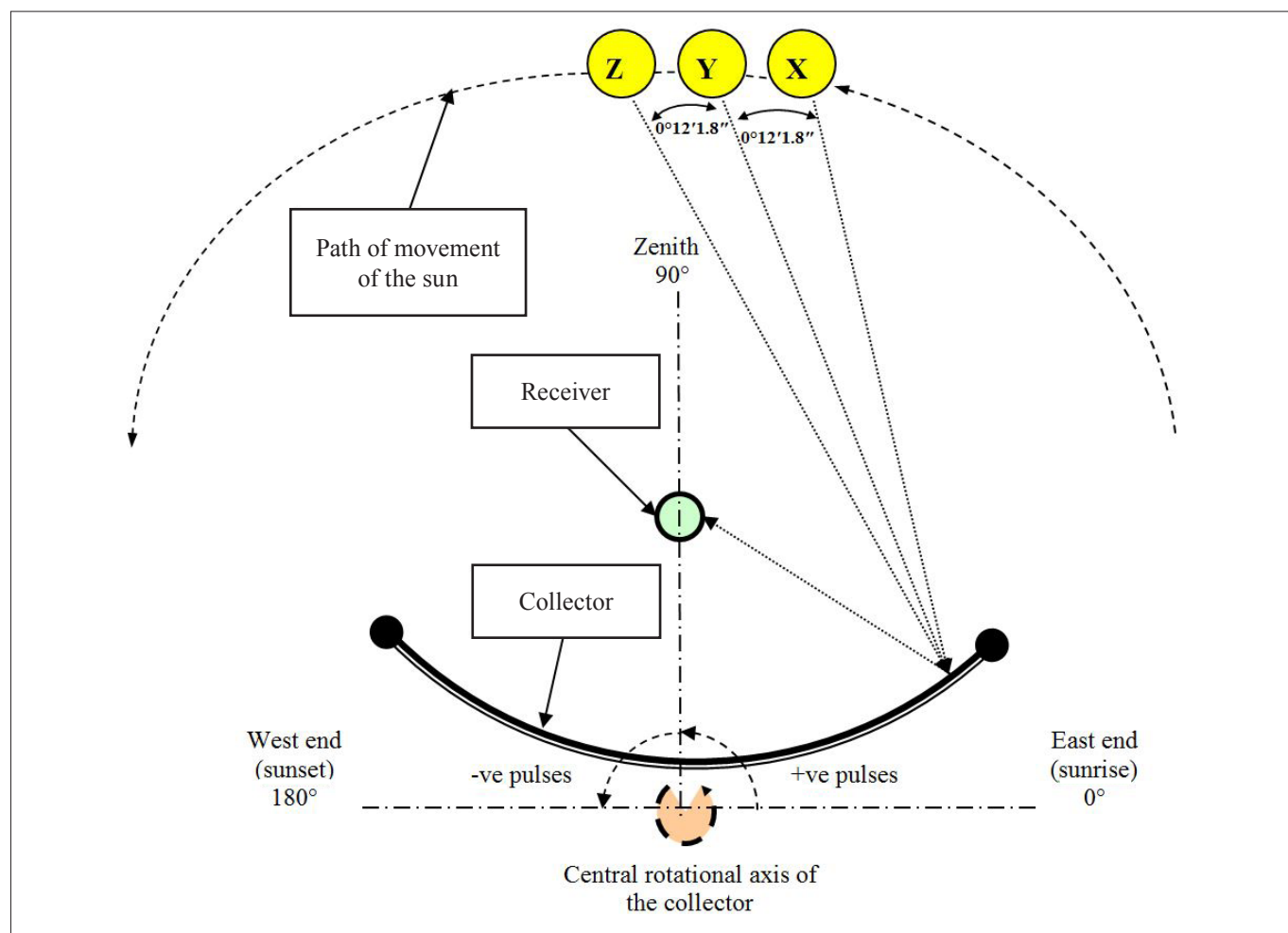
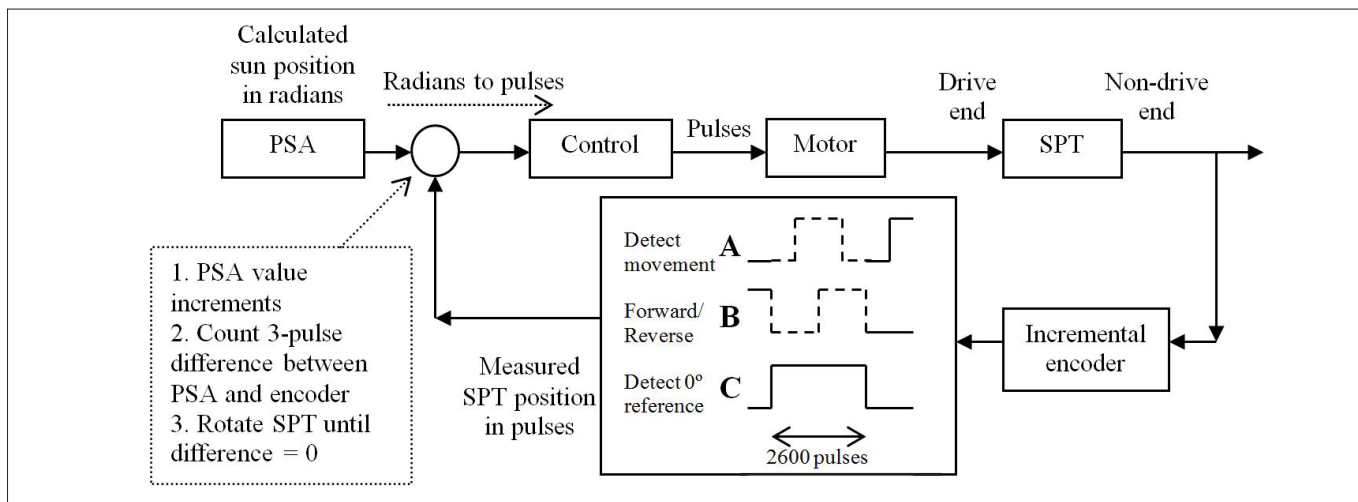


FIGURE 2: Rotational movement of the solar parabolic trough relative to the daily movement of the sun, as seen from the drive end of the trough.



PSA, Plataforma Solar de Almeria; SPT, solar parabolic trough.

FIGURE 3: Block diagram of the control algorithm.

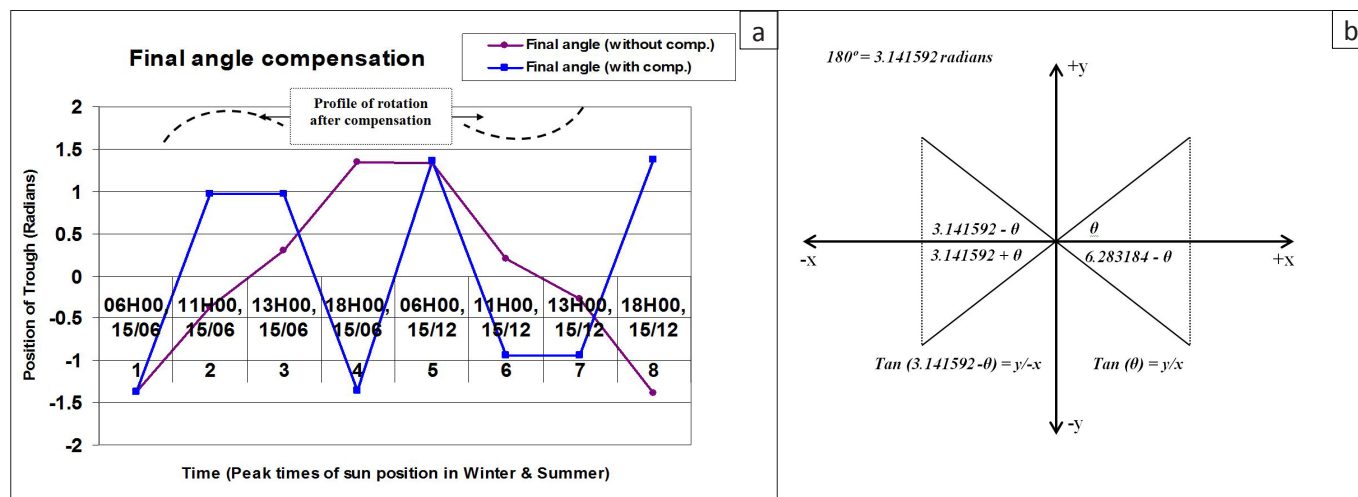


FIGURE 4: Determination of the final angle of the solar parabolic trough in the control software by (a) locating the correct quadrant for final angle calculation and (b) comparing the final angle before and after tangent compensation.

Compensation in the final angle to correct the SPT position

The angular values are expressed as radians in this section because the PLC Step7 software¹³ processes them in this format for correct angular position generated from the summing point of the controller to rotate the SPT (Figure 3).¹⁵ The PSA computation resulted in an acute angle (θ) for the SPT position from the tangent trigonometric ratio and specified whether the X- coordinates and Y-coordinates were negative or positive (Figure 4a). From the calculated coordinates the final angle was: θ in the 1st quadrant, $180^\circ - \theta$ in the 2nd quadrant, $180^\circ + \theta$ in the 3rd quadrant or $360^\circ - \theta$ in the 4th quadrant. It was essential to rotate the trough to the correct position by allowing the control algorithm to mathematically express the calculated value in the appropriate quadrant of the coordinate plane.

The eight plotted points were derived for peak winter and summer regions (Figure 4b and Table 1). The generated value was not necessarily correct as it may have existed in any of

the four quadrants of the Cartesian plane. All points represent the direct relationship between the generated answer before and after tangent compensation, indicating that points 1 and 5 commenced at the same value in each seasonal change but deviated with time. In winter, the angular value increased throughout the day, without compensation, and in summer it decreased.⁴ As the SPT rotated about its axis from the horizontal, 0-degree axis in the east position to the horizontal, 180-degree axis in the west position, the captured data with compensation represents a closer resemblance of this rotational movement. As a result of the variation in the sun's path with seasonal changes, as indicated in the rotational profile, a one-axis system requires further compensation. Seasonal effects on our one-axis, east-west system, resulted in an incorrect position of the SPT, especially in winter (Figure 5). In summer, there was a constant beam radiation from sunrise to sunset which allowed for constant solar-to-thermal conversion throughout the day (Figure 5a). In winter the beam radiation decreased towards midday, from sunrise to sunset, which decreased the solar-to-thermal conversion (Figure 5b). This resulted in partial reflected radiation from the collector onto the receiver,

TABLE 1: Analysis of the final angle before and after tangent compensation, as configured by the Siemens Step7 programmable logic controller software.

Point	Time	Season	Final angle (°)	
			Before configuration	After configuration
1	6:00	Mid-winter	-1.371466	-1.371344
2	11:00	Mid-winter	-0.372931	0.964857
3	13:00	Mid-winter	0.305941	0.961717
4	18:00	Mid-winter	1.346684	-1.358730
5	6:00	Mid-summer	1.327231	1.357530
6	11:00	Mid-summer	0.205971	-0.943463
7	13:00	Mid-summer	-0.276497	-0.943253
8	18:00	Mid-summer	-1.390707	1.368333

which reduced the solar-to-thermal conversion process. The reflected radiated beam had to be focused along the maximum longitudinal axis of the receiver, closest to the central point of the SPT, to decrease energy losses. As the SPT was fixed in the north-south position to track the sun in the east-west direction, an alternative method to compensate for this bias in winter had to be incorporated by introducing an offset.^{16,17} The geographical location of the SPT and seasonal changes resulted in an inverted angular position, which required an offset to optimise position control according to the Step7 PLC software.¹³

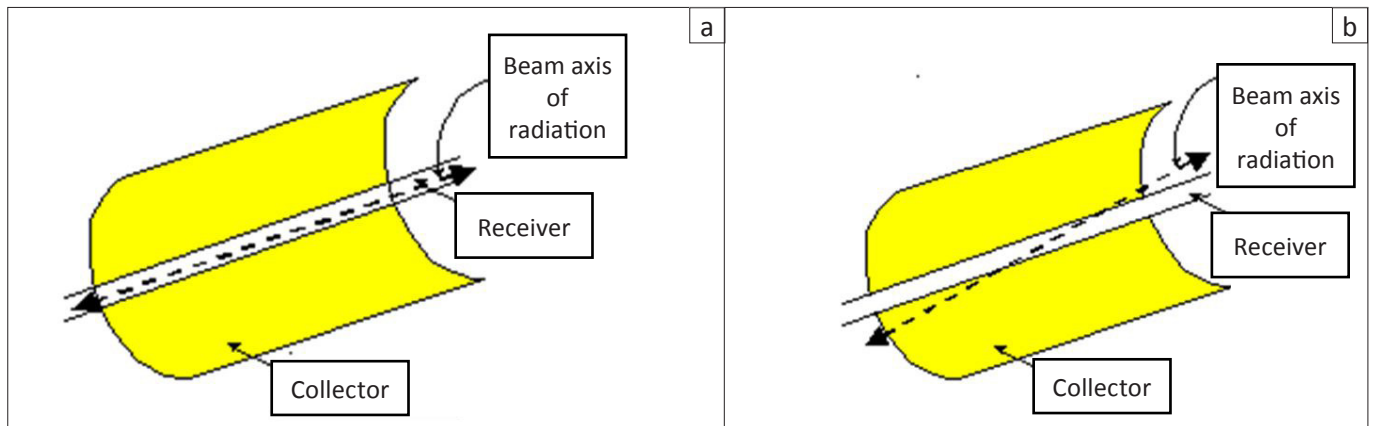
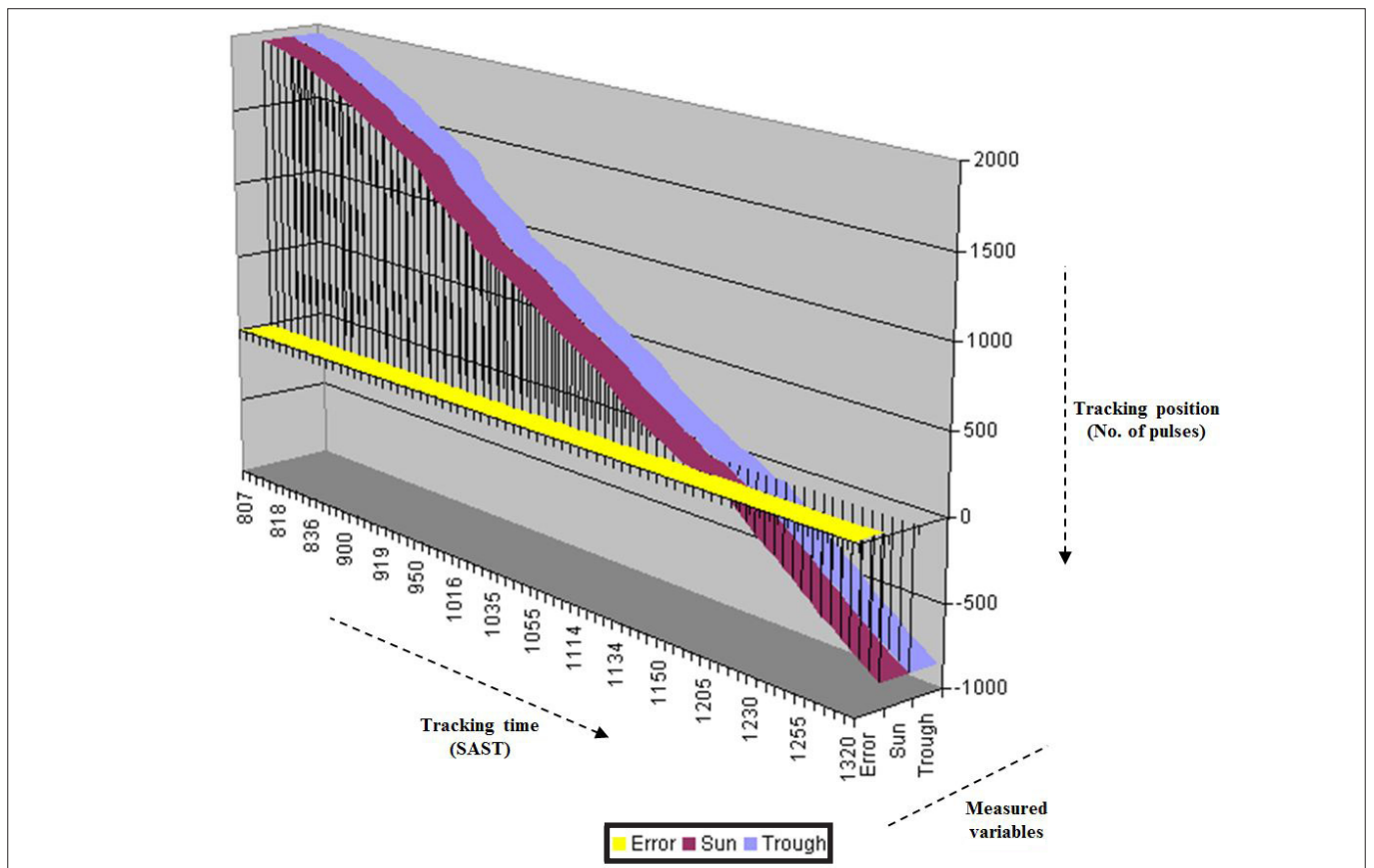


FIGURE 5: Effects of reflected radiation from the collector to the receiver as a result of seasonal changes in (a) summer and (b) winter.



SAST, South African Standard Time.

FIGURE 6: Implementation analysis to test the accuracy of the computed Plataforma Solar de Almeria (PSA) value and solar parabolic trough position with respect to the controller response.



Results and discussion

The calculated and measured values from the PSA computation and incremental encoder, respectively, are expressed as pulse counts in this section because the PLC software processes them in this format to generate a corrective output signal when there is a difference between the two input values at the summing point of the controller (Figure 3). The +2500 pulses, east position to the -2500 pulses, west position are represented on the z-axis (Figure 6). The tracking time in South African Standard Time (SAST) as captured in the PLC is represented on the x-axis. The three comparative variables – error signal, sun position and trough position – are represented on the y-axis. The error signal (an indication of the controller response) is the difference between the sun position (the computed value from the PSA calculation) and the trough position (measured from the encoder). As the computed PSA value varied with the sun's daily movement, the control algorithm measured the pulse count difference between the signals from the PSA computation and the incremental encoder (Figure 3). The measurable tolerance to meet the 0.007 radian limit was a three-pulse count to maintain the calculated 2.78 pulse according to the encoder specifications. The captured data ranged from +2000 pulses to -1000 pulses. Because the SPT commenced at the sunrise horizontal plane at +2000 pulses, east elevation and continued to rotate to the sunset horizontal plane at -1000 pulses, west elevation for the test condition, the actual vertical position at 11:50 was a 0-pulse signal. The trough was positioned in the east quadrant until 11:50, indicating all positive values, i.e. the sunrise side. In this quadrant the encoder signal of +2500 pulses to 0 pulses was representative of a movement from sunrise to the vertical position. After 11:50 the trough was positioned in the west quadrant, indicating all negative values, i.e. the sunset side. The pulsed signals were processed as negative values. In this quadrant the encoder signal of 0 pulses to -2500 pulses was representative of a movement from the vertical position to the sunset position (Figure 2 and Figure 6).^{2,3,5}

Conclusion

Both the trough position and sun position values varied by a constant amount, thereby allowing the trough to be focused in the path of the radiation of the sun for maximum reflection from the collector onto the receiver, for maximum absorption of solar energy to be converted to thermal energy. This phenomenon can be observed by the error signal being an almost straight line (indicating zero), along the x-axis, and the sun and trough positions decreasing from 2000 pulses to

-1000 pulses, along the z-axis. The error signal was precisely a maximum value of 3 pulses for optimal position of the parabolic trough, as processed in the software program, in keeping with the required tolerance of 0.007 radians (0° 24' 3.6").^{6,8,10}

Acknowledgements

We thank the Mangosuthu University of Technology, Eskom and the National Research Foundation (South Africa) for financial support; USAID, Siemens Automation & Drives and the Nelson Mandela Metropolitan University for equipment; and JVR Consulting Engineers for technical support.

References

1. Stine WB, Harrigan RW. Solar energy fundamentals and design. New York: Wiley; 1985.
2. Hurt R, Yim W, Boehm R, Hale MJ, Gee R. Advanced parabolic trough field testing – real-time data collection, archiving, and analysis for the solargenix advanced parabolic trough. Paper presented at: International Solar Energy Conference; 2006 July 08–13; Denver, Colorado; p. 1–6. Available from: <http://131.216.6.90/ceer/Portals/1/Publications/ISEC2006-99078.pdf>
3. Shortis MR, Johnston GHG, Pottler K, Lüpfer E. Remote sensing and spatial information sciences. *Int Arch Photogramm*. 2008;37(B5):81–87.
4. Geyer M, Lüpfer E, Osuna R, et al. EUROTROUGH – Parabolic trough collector developed for cost efficient solar power generation. Paper presented at: 11th International Symposium on Concentrating Solar Power and Chemical Energy Technologies; 2002 Sep 04–06; Zurich, Switzerland; p. 1–7.
5. Lüpfer E, Geyer M, Schiel W, et al. Eurotrough design issues and prototype testing at PSA. Paper presented at: Proceedings, Solar Forum, Solar Energy: The Power to Choose; 2001 Apr 21–25; Washington DC, USA. p. 1–5.
6. Reda I, Andreas A. Solar position algorithm for solar radiation applications. Technical report NREL/TP-560-34302. Washington DC: National Renewable Energy Laboratory; 2008; p. 1–12.
7. Kreith F, Kreider JF. Principles of solar engineering. New York: Hemisphere Publishing Corporation; 1978.
8. Gregg WW, Carder KL. A simple spectral solar irradiance model for cloudless maritime atmospheres. *Limnol Oceanogr*. 1990;35(8):1657–1675. doi:10.4319/lo.1990.35.8.1657
9. Solar energies technology program 2008–2012, multi-year program plan. Washington DC: US Department of Energy; 2008; p. 19–56.
10. Hegazy AS, ElMadany MM. Design and experimental testing of a solar parabolic trough collector with its tracking system for salt-water desalination in arid areas of Saudi Arabia. Paper presented at: Proceedings, 7th Saudi Engineering Conference; 2007 Dec 02–05; Riyadh, Saudi Arabia; p. 1–13.
11. Brooks MJ, Mills I, Harms T. Performance of a parabolic trough solar collector. *J Energy S Afr*. 2006;17(3):17–80.
12. Manuel BM, Diego CAP, Teodoro LM, Martin LC. Computing the solar vector. *Sol Energy*. 2001;70(5):431–441. doi:10.1016/S0038-092X(00)00156-0
13. Naidoo P. Intelligent control and tracking of a solar parabolic trough. PhD thesis, Port Elizabeth, Nelson Mandela Metropolitan University; 2006.
14. Pottler K, Lüpfer E, Johnston GHG, Shortis MR. Photogrammetry: A powerful tool for geometric analysis of solar concentrators and their components. *Trans ASME*. 2005;(127):94–101.
15. Berger H. Automating with Step7 in STL and SCL. Erlangen: Publicis MCD Verlag; 2000.
16. Washington State University Cooperative Extension Energy Program: Parabolic-trough solar collectors WSUCEEP00153. Pullman: Washington State University; 2003.
17. Boyle G. Renewable energy. Milton Keynes: The Open University; 2004.